Stabilization of a (3,0) mobile robot by means of an event-triggered control

Abstract

Event-triggered control is a sampling strategy that updates the control value only when some events related to the state of the system occurs. It therefore relaxes the periodicity of computations. This paper deals with the development of a nonlinear event-triggered control for the stabilization of a (3,0) mobile robot. Firstly, the existence of a stabilizing control law is proven and a Control Lyapunov Function (CLF) relative to the desired equilibrium (i.e. desired position) is obtained. Then, the construction of an event function and a feedback function is carried out. The event function is dependent on the time derivative of the CLF and the feedback function results from the extension of Sontag's general formula to event-triggered stabilization, which ensures asymptotic stability, smoothness everywhere and continuity at the equilibrium. Experimental results validate the theoretical analysis where a comparison with a computed torque control law is performed. Hence, the proposed scheme reduces the number of control updates, which implies a reduction of processor load without deteriorating the closed-loop performance. To the best of the authors' knowledge, this is the first time that such strategy is experimentally tested on a completely autonomous (3,0) mobile robot.

Keywords:

Event-triggered control, Control Lyapunov Function (CLF), (3,0) mobile robot.

1. Introduction

1.1. Motivations and Background

In recent years, the advances in Very Large Scale Integration (VLSI) in an integrated circuit have allowed the development of low-cost, low-power, small-sized computational elements. As a consequence, an increasing number of mechatronic systems includes embedded computers, which interact with the physical world through the use of sensors and actuators in order to exchange information. The integration of computation with physical processes results in Cyber-Physical Systems (CPS) [1] where the goal of this integration is to develop engineered systems that improves current systems with respect to autonomy, functionality, energy efficiency, usability, safety, and reliability. Unmanned Ground Vehicles (UGVs) include an important class of CPS where the intelligent interactions with the world, represents a challenge that needs to be taken into account [2–4].

Among UGVs, the holonomic omnidirectional vehicle (ODV) also known as (3,0) mobile robot, has caused great interest because of its high maneuverability [5–7]. Since this class of robot can execute holonomic movements, *i.e.* it can change its direction of movement without changing its orientation and without dramatically decreasing its speed, this robot is ideal in diverse applications such as security, automated transportation and logistics [8, 9] or even in the field of outdoor and rough terrain applications [10, 11].

Researches in control and robotics have proposed linear and nonlinear control approaches related to the stabilization and trajectory tracking problem of (3,0) mobile robots. The standard robot motion control have been designed either in a decentralized or in a centralized fashion [12, 13]. Decentralized control, also known as cascade

control, is based on the derived kinematic model [14], where the angular velocities of the actuators are the control inputs; and linear and angular velocities of the robots are the outputs. Then, each actuator is controlled separately, typically using a local velocity controller (see [15, 16] and references therein). On the other hand, centralized control is based on the dynamic robot model, similar to that proposed in the present paper, which is nonlinear and coupled. In this case, linear and nonlinear control laws have been developed using different approaches, *e.g.* feedback linearization (computed torque in robotics) [17], adaptive control [18], backstepping control [19], sliding mode control [20], LPV-based control [21], knowledge-based control [22], nonlinear model predictive control (NMPC) [23], GPI based observer control [24] and fuzzy control [25] where remarkable techniques can be used in order to provide robustness with respect to parameter uncertainties [26, 27]. This list is of course far from being exhaustive and within the previous mentioned approaches, the control design explicitly considers some coupling terms from the dynamics of the system. Therefore, it is expected to exhibit a better performance for high speed and acceleration profiles [28].

It is well known that when a continuous-time control law is implemented using a digital computer, the closed-loop system may not have the same stability properties as the system with a true continuous controller, due to delay and digitization errors [29]. Actually, all previously listed control laws were designed in a continuous-time framework and their implementation were carried out under embedded computers in the time-triggered framework, where the sampling time is constant. This procedure is called emulation and consists of implementing a continuous-time control algorithm with a constant and sufficiently small periodic sampling period [30]. Nevertheless, this procedure can be constrained by hardware (processor performance, cache hit percentage, memory latency, etc.) such that reducing the sampling period, to a level

that guarantees acceptable closed-loop performance, may be impossible in practice.

On the other hand, control techniques based on the discrete-time design have been widely studied lately, motivated by the remarkable technological advances in digital electronics [31]. In discrete-time control design, the discretization of the continuous-time plant model is made and then, the design of the controller based on the discrete plant model is carried out. The main advantage of the discrete-time control is that it does not require fast sampling rate and the designed controller always stabilizes the discrete plant [32]. The discrete-time control of linear systems is well understood and it is now a mature area [33]. Although efforts have been focused to extend them to nonlinear systems, the main drawback is to analytically obtain nonlinear exact discrete-time models, since it requires solving an explicit nonlinear initial value problem [30]. Therefore, the discrete-time control design requieres the approximate discrete-time model [34] to stabilize the approximate model of the plant but the discrete-time control could unstabilize the exact model. Then, the control redesign using Lyapunov-based, ISS (Input-to-State-Stability) and neural networks approaches are necessary in order to achieve the stabilization [35–37]. So far, much effort has been devoted to nonlinear discrete-time control design, but the proposed techniques remain complex for practical implementations.

In recent years, an interesting method known as Event-Based Control or Event-Triggered Control proposes to relax the sampling sequence by some events related to the state of the system. The idea arises in the context of Networked Control Systems (NCS) where the insertion of communication networks in the feedback control loops makes the analysis and synthesis of NCSs a challenge [38, 39]. Its main characteristic is that an event can be activated according to the system's dynamic behavior which indicates whether the control law is computed and applied to the system or not. Some works on event-based PID control have shown efficiency with a reduction of

control function calls [40–42]. Typical event-detection mechanisms are functions of the variation of the state or the output of the system, as is reported in [43–45]. Actually, the main difference among control strategies is the event function. In [46], the event function is related to the variation of the Lyapunov function and consequently to the state variable. The existence of a Lipschitz stabilizing control law, an Input to State Stable Control Lyapunov Function (ISS-CLF) and a Control Lyapunov Function (CLF) were proposed as event functions in [47, 48] and [49, 50], respectively. In [51], the event-triggered approach is stated for the estimation techniques of power systems based on Western Electric Rules and tracking state estimator.

Even though the benefits of event-based control have shown good results, few results in the framework of Unmanned Ground Vehicles (UGVs) have been reported. For instance, in [52] an event-based PID controller is proposed for velocity regulation. In [53] a distributed control algorithm based on event-triggered communications has been designed and implemented to bring the robots into the desired formation. In both works linear event-triggered controllers are proposed and the kinematic model was used for the control design, unlike in the present work. Furthermore, the control objectives are different.

1.2. Contributions

In the present work, an event-triggered nonlinear control law is proposed for the pose regulation of a (3,0) mobile robot. The control law is based on the dynamic robot model which can be written as an affine in the control dynamical system, such as is detailed in section 2. This section also presents an overview of the event-triggered strategy for the stabilization of nonlinear systems, proposed by one of the authors of this paper in [49]. Lemma 3.1 in section 3 is the first contribution

of this work. It presents the existence of a stabilizing control law and a Control Lyapunov Function (CLF) relative to the equilibrium $x_e = 0$. A version of a CLF relative to the equilibrium $x_e \neq 0$, where x_e is the desired pose, is given in remark 3.4. Remark 3.2 discloses that although the stabilizing control law presented in Lemma 3.1 can asymptotically stabilize the (3,0) mobile robot, the existence of this control law and the corresponding CLF is used here for the construction of the event function and the feedback function, such as is stated in Corollary 3.3. It is worth mentioning, that the event function is obtained from the time derivative of the CLF. Furthermore, the feedback function results from the extension of Sontag's general formula to event-triggered stabilization ensuring that the closed-loop system is asymptotically stable, smooth everywhere and continuous at the equilibrium. As was mentioned in [54], Sontag's formula possess robustness to static and dynamic input uncertainties. As a consequence, the proposed technique solves, implicitly, the problem of robust stabilization of a (3,0) mobile robot, which represents a second contribution. Finally, in section 4, the closed-loop system is carried out in real-time. It shows that such an event-triggered strategy reduces the number of control updates by 27.73 % and the power consumption, $w.r.t$ a continuous-time control law (computed torque with sampling time period fixed to 5 ms) without compromising the system's performance. To the best of the authors' knowledge, this is the first time that such a strategy is experimentally tested on a completely autonomous (3,0) mobile robot. This final point, represents the third and main contribution of this work.

2. Mathematical Background

In this section the dynamic model of the (3,0) mobile robot is briefly introduced. Furthermore, some aspects of nonlinear systems stabilization by means of an event-

triggered control are reviewed [49].

2.1. Dynamic model of the (3,0) mobile robot

According to the classification established in [6, 28] the (3,0) mobile robot is considered holonomic with three omnidirectional wheels providing three degrees of mobility and zero degree of steerability degree.

An isometric view of the mobile robot is shown in Fig. 1a. Two orthogonal right-hand coordinate systems are considered: an inertial coordinate system $\{w\}$ and a moving coordinate system $\{m\}$ with origin at the mass center of the robot. In Fig. 1b a photo of the mobile robot is given.

Let $x = (x_1\ x_2\ x_3\ x_4\ x_5\ x_6)^T = (x_w\ y_w\ \phi_w\ \dot{x}_w\ \dot{y}_w\ \dot{\phi}_w)^T$ denote the state vector corresponding to the linear and angular position and velocity of the omnidirectional mobile robot expressed in the inertial coordinate system and $u = (u_1\ u_2\ u_3)^T$ be the input torque vector generated by the wheels and following the procedure described in [17], then the dynamic model in the state variable representation is given by (1), where angles described between the axis Y_m and the axes of each wheel are represented by δ_1 and δ_3, $\bar{m}$ and I_z are the mass and the inertia of the mobile robot; r and J are the radius and the inertia of the wheels and L is the distance between the mass center of the mobile robot and the wheels.

$$\dot{x} = f(x) + g(x)u \tag{1}$$

where:

$$f(x) = \begin{pmatrix} x_4 & x_5 & x_6 & -\alpha_1 x_6 x_5 & \alpha_1 x_4 x_6 & 0 \end{pmatrix}^T$$

$$g(x) = \begin{pmatrix} 0 & 0 & 0 \\ 0 & 0 & 0 \\ 0 & 0 & 0 \\ -\alpha_2\beta_2 & 2\alpha_2 \sin x_3 & -\alpha_2\beta_1 \\ \alpha_2\beta_4 & -2\alpha_2 \cos x_3 & \alpha_2\beta_3 \\ \alpha_3 & \alpha_3 & \alpha_3 \end{pmatrix}$$

$$\begin{aligned} \alpha_1 &= \tfrac{3J}{2mr^2+3J} && ;\beta_1 = \sqrt{3}\cos x_3 + \sin x_3 \\ \alpha_2 &= \tfrac{r}{2mr^2+3J} && ;\beta_2 = \sin x_3 - \sqrt{3}\cos x_3 \\ \alpha_3 &= \tfrac{Lr}{3JL^2+I_z r^2} && ;\beta_3 = \cos x_3 - \sqrt{3}\sin x_3 \\ & && ;\beta_4 = \cos x_3 + \sqrt{3}\sin x_3 \end{aligned}$$

2.2. Event-triggered control

The study in this paper focuses on dynamical systems of the form

$$\dot{x} \;=\; f(x) + g(x)u \tag{2}$$

where $x \in \mathcal{X} \subset \mathbb{R}^n$, $u \in \mathcal{U} \subset \mathbb{R}^p$, f and g are smooth functions with f vanishing at the origin. For the sake of simplicity, in this paper only the case of null stabilization is considered. If the system admits an asymptotic stabilizing feedback $k : \mathcal{X} \to \mathcal{U}$ then there is a Control Lyapunov Function (CLF) $V : \mathcal{X} \to \mathbb{R}$, that is a smooth positive definite function such that:

$$\dot{V} = \frac{\partial V}{\partial x} f(x) + \frac{\partial V}{\partial x} g(x) k(x) \tag{3}$$

It is worth noting that if k is assumed to be smooth, then V exists and it is smooth. In the present work only the smoothness of V is required which is less restrictive.

The *event-triggered control* framework requires two functions:

- *Event function* $\bar{e} : \mathcal{X} \times \mathcal{X} \to \mathbb{R}$ that indicates if the control signal needs to be updated ($\bar{e} \leq 0$) or not ($\bar{e} > 0$). Event function $\bar{e}$ takes the current state x as input and a memory m of the vector x for the last time that $\bar{e}$ became negative.

- *Feedback function* $k : \mathcal{X} \to \mathcal{U}$, which is computed if the event function is activated.

Definition 2.1. *[49] An event-triggered feedback* $(k, \bar{e})$ *is said to be a semi-uniformly Minimal inter-Sampling Interval (MSI) if for all* $\delta > 0$ *and all* x_0 *in the ball of radius* δ *centered at the origin* $\mathcal{B}(\delta)$*, the time between two successive events can be lower bounded by a* $\underline{\tau} > 0$*.*

It is known that for a nonlinear system of the form (2) with a semi-uniformly MSI event-triggered control $(\bar{e}, k)$, the solution of equation (2) with initial conditions $x_0 \in \mathcal{X}$ in the time $t = 0$, is defined for all positive t as the solution of the differential system:

$$\dot{x} = f(x) + g(x)k(m) \tag{4}$$

$$\begin{cases} m = x & \text{if } \bar{e}(x, m) \leq 0,\ x \neq 0 \\ m = 0 & \text{elsewhere} \end{cases} \tag{5}$$

$$\text{with } x(0) := x_0 \text{ and } m(0) = x(0)$$

Theorem 2.2 (Event-triggered universal formula [49])**.** *If there exists a CLF for the system (2), then the event-based feedback* $(\bar{e}, k)$ *defined below is semiuniformly MSI,*

smooth on $\mathcal{X}\backslash\{0\}$*, and such that:*

$$\frac{\partial V}{\partial x} f(x) + \frac{\partial V}{\partial x} g(x) k(m) < 0, \quad x \in \mathcal{X}\backslash\{0\} \tag{6}$$

where m *is defined in (5) and* k *is:*

$$\begin{aligned} k_i(x) &:= -b_i(x)\delta_i(x)\gamma(x) \\ \bar{e}(x,m) &:= -a(x) - b(x)k(m) - \sigma\sqrt{a(x)^2 + \bar{\theta}(x)b(x)\Delta(x)b(x)^T} \end{aligned} \tag{7}$$

with

- $i \in \{1, 2, \ldots, p\}$,
- $a(x) := \frac{\partial V}{\partial x} f(x)$ *and* $b(x) := \frac{\partial V}{\partial x} g(x)$,
- $x \to \Delta(x) := diag(\delta_1(x), \delta_2(x), \ldots, \delta_p(x))$ *is a smooth function of* $\mathcal{X}\backslash\{0\}$ *to* $\mathbb{R}^{p\times p}$*, positive definite on:* $\mathcal{S} := \{x \in \mathcal{X} | \|b(x)\| \neq 0\}$,
- $x \to \bar{\theta}(x)$ *is a smooth positive function of* $\mathcal{X}$ *to* $\mathbb{R}$*, such that* $\bar{\theta}(x)\|\Delta(x)\|$ *vanishes at the origin and ensuring on* $\mathcal{S}\backslash\{0\}$ *the inequality* $a(x)^2 + \bar{\theta}(x)b(x)\Delta(x)b(x)^T > 0$,
- σ *is a control parameter that takes values in* $[0, 1)$,
- $\gamma : \mathcal{X} \to \mathbb{R}$ *is defined by:*

$$\gamma(x) := \begin{cases} \frac{a(x) + \sqrt{a(x)^2 + \bar{\theta}(x)b(x)\Delta(x)b(x)^T}}{b(x)\Delta(x)b(x)^T} & \text{if } x \in \mathcal{S} \\ 0 & \text{if } x \notin \mathcal{S} \end{cases} \tag{8}$$

Proof. The proof is presented in [49]. □

3. Design of control strategy

This section describes the design of an event-triggered control for the stabilization of the (3,0) mobile robot. For this purpose, a CLF is first obtained to the nonlinear system (1). The objective consists of finding the pair $u = \bar{k}(x)$ and V such that the following asymptotic condition is fulfilled:

$$\lim_{t\to\infty} x(t) = x_e = \mathbf{0} \text{ and } \frac{\partial V}{\partial x} f(x) + \frac{\partial V}{\partial x} g(x)\bar{k}(x) < 0 \tag{9}$$

where $\mathbf{0} \in \mathbb{R}^6$ is the origin of the space state. In the case that the desired equilibrium (robot's desired position) is $x_e \neq 0$, the variable change $z = x - x_e$ must be considered for the stabilizing feedback and the asymptotic condition becomes:

$$\lim_{t\to\infty} z(t) = \mathbf{0} \text{ and } \frac{\partial V}{\partial z} f(z) + \frac{\partial V}{\partial z} g(z)\bar{k}(z) < 0 \tag{10}$$

Once the existence of a stabilizing control $u = \bar{k}(x)$ (respectively, $u = \bar{k}(z)$) and a CLF $V(x)$ (respectively, $V(z)$) is proven, the event-triggered control will be developed.

With the above requirements, our first result is the following:

Lemma 3.1. *Consider the function $V : \mathbb{R}^6 \to \mathbb{R}$ defined by:*

$$\begin{aligned} V(x) = & P_1 x_1^2 + P_2 x_2^2 + P_3 x_3^2 + P_4 x_4^2 + P_5 x_5^2 \\ & + P_6 x_6^2 + 2P_7 x_1 x_4 + 2P_8 x_2 x_5 + 2P_9 x_3 x_6 \end{aligned} \tag{11}$$

with $P_{i+1} = \sqrt{\varrho_{i+1}\varrho_{i+4} + 2\sqrt{\varrho_{i+1}^3/\epsilon_{i+1}}}$, $P_{i+4} = \sqrt{\varrho_{i+4}/\epsilon_{i+1} + \sqrt{4\varrho_{i+1}/\epsilon_{i+1}^3}}$, $P_{i+7} = \sqrt{\varrho_{i+1}/\epsilon_{i+1}}$, where $\epsilon_{i+1}, \varrho_{i+1}, \varrho_{i+4} \in \mathbb{R}^+ \ \forall \ i = 0, 1, 2$. Then, (11) is a CLF for the system (1) relative to the equilibrium state $x_e = \boldsymbol{0} \in R^6$ with the stabilizing control

$u = \bar{k}(x) \in \mathbb{R}^3$ *defined by:*

$$\begin{aligned}
\bar{k}_1=&\frac{1}{12}\beta_2\frac{\epsilon_1}{\alpha_2}P_7x_1 - \frac{1}{6}\frac{\epsilon_3}{\alpha_3}P_6x_6 - \frac{1}{2}\frac{J}{r}\beta_2x_5x_6 - \frac{1}{2}\frac{J}{r}\beta_4x_4x_6 - \frac{1}{6}\frac{\epsilon_3}{\alpha_3}P_9x_3 \\
&+\frac{1}{12}\beta_2\frac{\epsilon_1}{\alpha_2}P_4x_4 - \frac{1}{12}\beta_4\frac{\epsilon_2}{\alpha_2}P_8x_2 - \frac{1}{12}\beta_4\frac{\epsilon_2}{\alpha_2}P_5x_5 \qquad (12)\\
\bar{k}_2=&\frac{J}{r}x_4x_6\cos x_3 - \frac{1}{6}\frac{\epsilon_3}{\alpha_3}P_6x_6 - \frac{1}{6}\frac{\epsilon_3}{\alpha_3}P_9x_3 + \frac{J}{r}x_5x_6\sin x_3 + \frac{1}{6}\frac{\epsilon_2}{\alpha_2}P_8x_2\cos x_3 \\
&+\frac{1}{6}\frac{\epsilon_2}{\alpha_2}P_5x_5\cos x_3 - \frac{1}{6}\frac{\epsilon_1}{\alpha_2}P_7x_1\sin x_3 - \frac{1}{6}\frac{\epsilon_1}{\alpha_2}P_4x_4\sin x_3 \qquad (13)\\
\bar{k}_3=&\frac{1}{12}\beta_1\frac{\epsilon_1}{\alpha_2}P_7x_1 - \frac{1}{6}\frac{\epsilon_3}{\alpha_3}P_6x_6 - \frac{1}{2}\frac{J}{r}\beta_1x_5x_6 - \frac{1}{2}\frac{J}{r}\beta_3x_4x_6 - \frac{1}{6}\frac{\epsilon_3}{\alpha_3}P_9x_3 \\
&+\frac{1}{12}\beta_1\frac{\epsilon_1}{\alpha_2}P_4x_4 - \frac{1}{12}\beta_3\frac{\epsilon_2}{\alpha_2}P_8x_2 - \frac{1}{12}\beta_3\frac{\epsilon_2}{\alpha_2}P_5x_5 \qquad (14)
\end{aligned}$$

Proof. It is clear that Lyapunov function V is smooth, positive definite and proper for $P_j \in \mathbb{R}^+ \ \forall \ j = 1, 2, ..., 9$. This Lyapunov function can be rewritten as follows:

$$
\begin{aligned}
V(x) \quad &= P_7\sqrt{\epsilon_1}\sqrt{2P_7}x_1^2 + P_7\left(\frac{\sqrt{2P_7}-\sqrt{P_7}}{\sqrt{\varrho_1}}\right)x_4^2 \\
&+P_7\left({}^4\sqrt{P_7\epsilon_1}x_1 + {}^4\sqrt{\frac{P_7}{\varrho_1}}x_4\right)^2 - P_7\sqrt{\epsilon_1}\sqrt{P_7}x_1^2 \\
&+P_8\sqrt{\epsilon_2}\sqrt{2P_8}x_1^2 + P_8\left(\frac{\sqrt{2P_8}-\sqrt{P_8}}{\sqrt{\varrho_2}}\right)x_4^2 \\
&+P_8\left({}^4\sqrt{P_8\epsilon_2}x_1 + {}^4\sqrt{\frac{P_8}{\varrho_2}}x_4\right)^2 - P_8\sqrt{\epsilon_2}\sqrt{P_8}x_1^2 \\
&+P_9\sqrt{\epsilon_3}\sqrt{2P_9}x_1^2 + P_9\left(\frac{\sqrt{2P_9}-\sqrt{P_9}}{\sqrt{\varrho_3}}\right)x_4^2 \\
&+P_9\left({}^4\sqrt{P_9\epsilon_3}x_1 + {}^4\sqrt{\frac{P_9}{\varrho_3}}x_4\right)^2 - P_9\sqrt{\epsilon_3}\sqrt{P_9}x_1^2 \qquad (15)
\end{aligned}
$$

Then, evaluating the time derivative of $V(x)$ along the trajectories of (1), one obtains

$$
\begin{aligned}
\dot{V}(x) &= 2P_1x_1\dot{x}_1 + 2P_2x_2\dot{x}_2 + 2P_3x_3\dot{x}_3 + 2P_4x_4\dot{x}_4 + 2P_5x_5\dot{x}_5 + 2P_6x_6\dot{x}_6 \\
&+ 2P_7\dot{x}_1x_4 + 2P_7x_1\dot{x}_4 + 2P_8\dot{x}_2x_5 + 2P_8x_2\dot{x}_5 + 2P_9\dot{x}_3x_6 + 2P_9x_3\dot{x}_6 \\
&= (2P_1x_1 + 2P_7x_4)\,x_4 + (2P_2x_2 + 2P_8x_5)\,x_5 - (2P_4x_4 + 2P_7x_1) \\
&(\alpha_2\beta_1u_3 + \alpha_1x_5x_6 + \alpha_2\beta_2u_1) + (2P_5x_5 + 2P_8x_2) \qquad (16) \\
&(\alpha_2\beta_4u_1 + \alpha_2\beta_3u_3 - \alpha_1x_4x_6) + (2P_4x_4 + 2P_7x_1)\,2\alpha_2u_2\sin x_3 \\
&+ (2P_3x_3 + 2P_9x_6)\,x_6 - (2P_5x_5 + 2P_8x_2)\,2\alpha_2u_2\cos x_3 \\
&+ (2P_6x_6 + 2P_9x_3)\,(\alpha_3\,(u_1 + u_2 + u_3))
\end{aligned}
$$

Including the control law (12)-(14) in (16), the time derivative of the Lyapunov function becomes:

$$
\begin{aligned}
\dot{V}(x) = & -\epsilon_1 P_7^2 x_1^2 - \epsilon_2 P_8^2 x_2^2 - \epsilon_3 P_9^2 x_3^2 + \left(2P_7 - \epsilon_1 P_4^2\right) x_4^2 \\
& + \left(2P_1 - 2\epsilon_1 P_4 P_7\right) x_1 x_4 + \left(2P_2 - 2\epsilon_2 P_5 P_8\right) x_2 x_5 \\
& + \left(2P_8 - \epsilon_2 P_5^2\right) x_5^2 + \left(2P_9 - \epsilon_3 P_6^2\right) x_6^2 + \left(2P_3 - 2\epsilon_3 P_6 P_9\right) x_3 x_6 \\
& = -\varrho_1 x_1^2 - \varrho_2 x_2^2 - \varrho_3 x_3^2 - \varrho_4 x_4^2 - \varrho_5 x_5^2 - \varrho_6 x_6^2 < 0 \ \forall \ x \neq 0
\end{aligned} \tag{17}
$$

Hence, the nonlinear system (1) with the control system (12)-(14) is asymptotically stable with a domain of attraction equal to $\mathbb{R}^6 \backslash 2n\pi \ \forall \ n = 0, 1, ..., \infty$. Accordingly, V is a CLF for (1) relative to the equilibrium state $x_e = \mathbf{0}$. □

Remark 3.2. *Note that Lemma 3.1 shows the existence of a stabilizing control law and a CLF. However, the control law (12)-(14) is not used anymore. Instead, the event-based feedback designed in the next subsection is applied to the system. Actually, the event function and the event-based feedback function depends on the CLF (11).*

3.1. Event-triggered control for (3,0) mobile robot

Given the CLF (11) associated with the system (1), the event-triggered control technique described in (2.2) can be applied and one can state the following result.

Corollary 3.3. *Considering the dynamics of the (3,0) mobile robot defined in (1) and the CLF given in (11), then, the event-triggered control $u = k(m)$ defined in (18) with the event $\bar{e}(x, m)$ (19), asymptotically stabilizes the (3,0) mobile robot at the origin. In addition, the control $(u, \bar{e})$ is semi-uniform MSI and smooth in $\mathbb{R}^6 \backslash \{0\}$.*

$$
k(m) = -b(x)\delta(x)\gamma(x) \tag{18}
$$

$$
\bar{e}(x, m) = -a(x) - b(x)k(m) - \sigma\sqrt{a(x)^2 + \bar{\theta}(x)b(x)\Delta(x)b(x)^T} \tag{19}
$$

where $a(x) \in R$ *and* $b(x) = (b_1 \ b_2 \ b_3) \in R^{1\times 3}$ *are given by:*

$$\begin{aligned}
a(x) \quad &= 2P_8x_5^2 + 2P_9x_6^2 - 2\alpha_1 P_5 x_4 x_5 x_6 + 2P_2 x_2 x_5 \\
&\quad +2P_3 x_3 x_6 - 2\alpha_1 P_4 x_4 x_5 x_6 + 2P_1 x_1 x_4 \\
&\quad -2\alpha_1 P_7 x_1 x_5 x_6 - 2\alpha_1 P_8 x_2 x_4 x_6 + 2P_7 x_4^2 \qquad (20) \\
b_1 \quad &= 2\alpha_3 P_6 x_6 + 2\alpha_3 P_9 x_3 - 2\alpha_2\beta_2 P_4 x_4 - 2\alpha_2\beta_2 P_7 x_1 \\
&\quad +2\alpha_2\beta_4 P_5 x_5 + 2\alpha_2\beta_4 P_8 x_2 \qquad (21) \\
b_2 \quad &= 2\alpha_3 P_9 x_3 - 4\alpha_2 P_5 x_5 \cos x_3 - 4\alpha_2 P_8 x_2 \cos x_3 \\
&\quad +4\alpha_2 P_4 x_4 \sin x_3 + 4\alpha_2 P_7 x_1 \sin x_3 + 2\alpha_3 P_6 x_6 \qquad (22) \\
b_3 \quad &= 2\alpha_3 P_9 x_3 - 2\alpha_2\beta_1 P_4 x_4 - 2\alpha_2\beta_1 P_7 x_1 \\
&\quad +2\alpha_2\beta_3 P_5 x_5 + 2\alpha_2\beta_3 P_8 x_2 + 2\alpha_3 P_6 x_6 \qquad (23)
\end{aligned}$$

The proof of Corollary 3.3 follows the one of Theorem 2.2. However, it is important to highlight the advantages and properties of the control law (18) and the rationale behind the construction of the event function (19).

- First, the feedback (7) is based on the general formula for the stabilization of nonlinear systems proposed by E. Sontag in [55] in the continuous framework. In [49] is extended the results to the event-triggered framework and it is shown that this control law is smooth everywhere and continuous at the origin.

- The problem of robust stabilization of nonlinear systems in the presence of input uncertainties is of great importance in practical implementation. Stabilizing control laws may not be robust to this type of uncertainty, especially if cancellation of nonlinearities is used in the design, *e.g.* control laws based

on feedback linealization as this one of the computed torque in robotics. As was mentioned in [54], Sontag's formula possess robustness to static and dynamic input uncertainties. As a consequence, the proposed technique solves, implicitly, the problem of robust stabilization of a (3,0) mobile robot.

- There are no systematic techniques for finding CLFs for general nonlinear systems, but the proposed approach can be applied successfully to holonomic omnidirectional vehicles *i.e.* (3,0) mobile robots, whose CLFs can be found.

- The rationale behind the construction of feedback (8) is the following [49]. In the event function the term $a(x)+b(x)k(m)$ is the time derivative of V, whereas $-\sqrt{a(x)^2+\bar{\theta}(x)b(x)\Delta(x)b(x)^T}$ is the value of $\dot{V}$ if $k(x)$ is used instead of $k(m)$. Therefore, right after an event, the event function presents a positive value $(\bar{e}(x,m) = (1-\sigma)\sqrt{a(x)^2+\bar{\theta}(x)b(x)\Delta(x)b(x)^T} > 0,\ \sigma \in [0,1[)$ and remains positive as long as $\dot{V} \leq \sigma\sqrt{a(x)^2+\bar{\theta}(x)b(x)\Delta(x)b(x)^T}$. Events will be more frequent with smaller σ. Then, σ results in a tuning parameter. The second tuning parameter, of the control law, is the function $\Delta(x)$ that directly impacts the performance of the control as well as the frequency of events.

Remark 3.4. *Note that the control system is performed for null stabilization i.e* $x_e = x = 0$. *In the case that the equilibrium is* $x_e \neq 0$, *a variable change* $(z = x - x_e)$ *must be considered for the stabilizing feedback and the CLF must be changed to* $V(z) = P_1z_1^2 + P_2z_2^2 + P_3z_3^2 + P_4z_4^2 + P_5z_5^2 + P_6z_6^2 + 2P_7z_1z_4 + 2P_8z_2z_5 + 2P_9z_3z_6$.

4. Real-time experimentation

The aim of this section is to show the effectiveness of the proposed event-triggered control for the stabilization of the (3,0) mobile robot, hence Real-time experiments on the (3,0) mobile robot prototype (Fig. 1) are carried out.

This mechatronic prototype was designed and developed using optimization techniques in order to maximize the dexterity of the mobile robot by properly locating the omnidirectional wheels [7]. The mobile robot includes a Mini-ITX GA-D425TUD mother board with Intel Atom D525, an embedded data acquisition system "Sensoray 626" and DC motor's drivers "Advanced Motion model 12A8" to compute the control law and to interact with sensors and actuators. Two lead-acid battery 12V/12A supply the power to the hardware of the mobile robot. The control law is programmed in Simulink program with Real-Time Windows Target for executing simulink models with a real-time kernel in Windows. An odometry system [16] is used to obtain the state vector x (position and velocity) at 200 Hz (*i.e.* the sample time is chosen as $\Delta t = 5ms$).

The event-triggered control strategy for the stabilization problem is represented in the block diagram of Fig. 2. The solid lines within the cyber system, indicate a continuous (periodic) information flow and the dashed lines denote that the information flow is only transmitted when there is an event function. The odometry system continuously calculates the state vector x. The state vector z is obtained by using the state vector x, the desired position x^d and the variable change $z = T(x) = x - x^d$. Based on the current state information z_i and the last computed control signal $u = k(m)$ stored in memory, the event function can be computed. The event function decides when to call the control function. The control function takes into account the current state information z_i as input argument. Whenever the control function receives a new state value z_i, it updates the control law $u = k(m)$ and the new value of the control signal is returned and stored in the memory. Then, the stored control signal value is used to change or to keep the PWM signals and moreover to evaluate the next event-triggered function for detecting a new event. Thus, the experiment consists in showing the performance of the mobile robot position by

means of an event-triggered feedback, *i.e.* with the control law (18) together with the event function (19). The motivation is to show the reduction of computation load (arithmetic operation, data storage and transfer of information) with respect to the time-triggered framework. Note that the saved computational resources (thanks to an event-based approach) could be used to process other information within the embedded system for instance, Inertia Measurement Unit (IMU), Global Positioning System (GPS), laser sensors, video, etc.

The experimental results consider the initial condition of the mobile robot as the origin, i.e., $x(0) = (0\ 0\ 0\ 0\ 0\ 0)^T$. Four different positions in the Cartesian space are considered as the desired positions that must be reached by the mobile robot in sequential order. These positions are $Q_1 : x^d = (0\ 0.7\ 0.2\ 0\ 0\ 0)^T$, $Q_2 : x^d = (0.7\ -0.7\ 0.5\ 0\ 0\ 0)^T$, $Q_3 : x^d = (-0.7\ -0.7\ 1\ 0\ 0\ 0)^T$, $Q_4 : x^d = (0\ 0.7\ 1.2\ 0\ 0\ 0)^T$. These positions must be reached at a maximum time of 30 s and then, the experimental results will be carried out at a final time of $t_f = 120s$.

In order to compare the control performance of the proposed event-triggered control (ETC) and to evaluate its advantages, the computed torque control (CTC) [17] is implemented. The technical specifications of the omnidirectional mobile robot prototype are stated in Table I. The control parameters $\epsilon \in R^3$ and $\varrho \in R^6$ of the ETC are proposed as follows: : $\varrho_1 = \varrho_2 = 6.4431e3$, $\varrho_3 = \varrho_6 = 35.0237$, $\varrho_4 = \varrho_5 = 35.0237$, $\epsilon_1 = \epsilon_2 = 6.20e-4$ and $\epsilon_3 = 0.0999$. Those parameters consider large positive values of the Lyapunov function. The frequency of the events is driven by σ, which is set to $\sigma = 0.9$. Furthermore, $\bar{\theta} = b(x)\Delta(x)b(x)^T - 2a(x)$ and $\Delta(x) = \text{diag}(0.01, 0.01, 0.01) \in \mathbb{R}^{3\times3}$.

The proportional and derivative gains of the CTC are established as: $k_{p_1} = 50$, $k_{d_1} = 5$, $k_{p_2} = 100$, $k_{d_2} = 170$, $k_{p_3} = 590$, $k_{d_3} = 10$. It is important to note that the selection of the CTC gains is based on having a similar closed-loop performance as

the obtained in the ETC.

In Fig. 3a the behavior of the (3,0) mobile robot in the plane $X_w - Y_w$ is shown for both control strategies and in Fig. 3b-3d the linear position and the angular position of the mobile robot are separately presented. In order to carry out an analysis of performance of the closed-loop system, three different control performance indexes are considered: the Integral Absolute Error (IAE), the Integral Time-weighted Absolute Error (ITAE) and the Integral Squared Error (ISE). In Table II those performance indexes are displayed for each degree of freedom d.o.f. (x_w, y_w, ϕ_w). It is clear that both control approaches present a similar performance and the position error in the experimental results converge to a value near to zero. In spite of the asynchronous activation of the control system in the ETC, it does not deteriorate the closed loop performance.

On the other hand, in Fig 4 the control signal behavior for both strategies are presented. In the last column of Table II the total torque is evaluated. It is observed that the ETC requires less applied torque to actuators (DC motors) than the CTC, in spite of presenting similar closed-loop performance. As the applied torque is related to the provided energy, the ETC requires less energy consumption to the actuators.

The Lyapunov function is presented in Fig. $5a$ where it is possible to observe that it converges around the zero value when the system stabilizes at the desired position and the same happens with the event function evolution shown in Fig. $5b$. Finally, Fig. $5c$ represents the event function activation flag, where "1" indicates that the control system is computed, updated and applied ($\bar{e} \leq 0$) and "0" represents that the control system is taken from the previous computed control value stored in memory ($\bar{e} > 0$). Note that with the CTC, which is based on time-triggered control, the control signal should be computed at each sampling time $\Delta t = 5ms$, hence $24,000$ updates of the control law is required for the previous experiment

with a final time of $t_f = 120s$. Meanwhile, with the ETC only 18303 updates are required due to the asynchronous activation of the event function (see Fig. $5c$). Considering the difference between the updates of the ETC and CTC, the proposed control approach reduces by 23.73% the update of the control signal compared with the CTC, which implies a decrease in arithmetic operations, data storage and transfer of information. The decrease of three such factors reduces the energy required to perform the updating. In spite of the asynchronous activation of the control signal in the ETC, the stability of the closed-loop system is guaranteed. Moreover, the computing time to evaluate the control law (18) is $7.84\mu s$, meanwhile the computing time required for evaluating the event-function is $6.35\mu s$. Hence $1.49\mu s$ is reduced for each inactivation of the event function activation flag. Therefore, with the ETC the computational load is diminished around $8.48ms$ for the particular experiment.

5. Conclusion

In this paper, the development and implementation of a nonlinear event-triggered feedback for the position stabilization of a (3,0) mobile robot is presented. Firstly, using a stabilizing control, the existence of a smooth CLF for the dynamics of the mobile robot is proven. Secondly, an event-triggered control is derived from the CLF function by considering the universal formula for event-triggered stabilization of general nonlinear systems affine in the control. The control law ensures, theoretically, the asymptotic stability of the closed-loop system to the desired position. An experimental prototype is used in order to validate the proposed strategy in real-time. The experiments show that the event based controller significatively reduces the number of times of control functions calls without deteriorating the closed-loop system performance, which results in energy saving in arithmetic operations, data storage and transfer of information; the decrease of the torque applied to the actuators and the

reduction of the computational load. However, thanks to the asynchronous control, the proposed approach allows the possibility of being implemented in embedded systems to operate with low power consumption. Outdoor real-time implementation and tracking trajectories will be addressed in the future.

Acknowledgment

The first author acknowledges support from the COFAA of the Instituto Politécnico Nacional and from SEP-CONACyT, via the project numbers 20140926 and 182298, respectively. The second author acknowledges support from the Vicerrectoría de Investigación y Estudios de Posgrado de la BUAP, via the project number GUCJING13-I. The third author acknowledge support from the Mexican Consejo Nacional de Ciencia y Tecnología (CONACyT) through a scholarship to pursue graduate studies at BUAP. The fourth author acknowledge support from the Universidad Politécnica de Puebla and the Programa para el Desarrollo Profesional Docente to pursue postgraduate studies at CIDETEC-IPN.

References

[1] E. A. Lee, S. A. Seshia, Introduction to Embedded Systems - A Cyber-Physical Systems Approach, Lee and Seshia, 2010.

[2] J. Clark, R. Fierro, Mobile robotic sensors for perimeter detection and tracking, ISA Transactions 46 (1) (2007) 3 – 13.

[3] G. Meirion-Griffith, M. Spenko, An empirical study of the terramechanics of small unmanned ground vehicles, in: Proc. of the IEEE Aerospace Conference, 2010, pp. 1–6.

[4] M. S. Miah, W. Gueaieb, Mobile robot trajectory tracking using noisy RSS measurements: An RFID approach, ISA Transactions 53 (2) (2014) 433 – 443.

[5] F. Pin, S. Killough, A new family of omnidirectional and holonomic wheeled platforms for mobile robots, IEEE Transactions on Robotics and Automation, 10 (4) (1994) 480–489.

[6] G. Campion, G. Bastin, B. Dandrea-Novel, Structural properties and classification of kinematic and dynamic models of wheeled mobile robots, IEEE Transactions on Robotics and Automation 12 (1) (1996) 47–62.

[7] M. G. Villarreal-Cervantes, C. Cruz-Villar, J. Álvarez Gallegos, E. Portilla-Flores, Kinematic dexterity maximization of an omnidirectional wheeled mobile robot: A comparison of metaheuristic and SQP algorithms, International Journal of Advanced Robot System 9 (161) (2012) 1–7.

[8] M. Wada, H. Asada, Design and control of a variable footprint mechanism for holonomic omnidirectional vehicles and its application to wheelchairs, IEEE Transactions on Robotics and Automation 15 (6) (1999) 978–989.

[9] F. Kuenemund, C. Kirsch, D. Hess, C. Roehrig, Fast and accurate trajectory generation for non-circular omnidirectional robots in industrial applications, in: Proceedings of ROBOTIK 2012; 7th German Conference on Robotics, 2012, pp. 1–6.

[10] M. Udengaard, K. Iagnemma, Design of an omnidirectional mobile robot for rough terrain, in: Proc. of the IEEE Conference on Robotic and Automation (ICRA), 2008, pp. 1666–1671.

[11] C. Nie, M. Assaliyski, M. Spenko, Design and experimental characterization of an omnidirectional unmanned ground vehicle for unstructured terrain, Robotica FirstView (2014) 1–17. doi:10.1017/S0263574714001180.

[12] C. Canudas de Wit, B. Siciliano, G. Bastin, Theory of Robot Control, Springer-Verlag, 1996.

[13] L. Sciavicco, B. Siciliano, Modelling and Control of Robot Manipulators, 2nd Edition, Germany: Springer-Verlag, 2000.

[14] S. K. Saha, J. Angeles, J. Darcovich, The design of kinematically isotropic rolling robots with omnidirectional wheels, Mechanism and Machine Theory 30 (8) (1995) 1127 – 1137.

[15] G. Indiveri, Swedish wheeled omnidirectional mobile robots: Kinematics analysis and control, IEEE Transactions on Robotics 25 (1) (2009) 164–171.

[16] J. Guerrero-Castellanos, M. Villarreal-Cervantes, J. Sánchez-Santana, S. Ramírez-Martínez, Trajectory tracking of a mobile robot (3,0) by means of bounded control, Revista Iberoamericana de Automática e Informática Industrial RIAI 11 (4) (2014) 426 – 434.

[17] B. R., A. Ghosal, Modelling of slip for wheeled mobile robots, IEEE Transactions on Robotics and Automation 11 (1) (1995) 126–132.

[18] H.-C. Huang, C.-C. Tsai, Adaptive robust control of an omnidirectional mobile platform for autonomous service robots in polar coordinates, Journal of Intelligent and Robotic Systems 51 (4) (2008) 439–460.

[19] S.-H. Chen, J. C. Juang, S.-H. Su, Backstepping control with sum of squares design for omni-directional mobile robots, in: International Conference on Control Automation and Systems (ICCAS-SICE), 2009, pp. 545–550.

[20] P. H. K. Khanh, N. T. Trung, P. T. Doan, N. Hung, Trajectory tracking control of omnidirectional mobile robot using sliding mode controller, in: International Conference on Control Automation and Systems (ICCAS), 2013, pp. 1170–1175.

[21] D. Rotondo, F. Nejjari, V. Puig, Model reference switching quasi-lpv control of a four wheeled omnidirectional robot, in: Proc. of the World Congress, The International Federation of Automatic Control (IFAC), 2014, pp. 4062–4067.

[22] A. da Costa, A. Ceonceicao, R. Cerqueira, T. Ribeiro, Omnidirectional mobile robots navigation: A joint approach combining reinforcement learning and knowledge-based systems, in: Biosignals and Biorobotics Conference (BRC), 2013, pp. 1–6.

[23] T. Teatro, J. Eklund, R. Milman, Nonlinear model predictive control for omnidirectional robot motion planning and tracking with avoidance of moving obstacles, Canadian Journal of Electrical and Computer Engineering, 37 (3) (2014) 151–156.

[24] C. Ren, S. Ma, Generalized proportional integral observer based control of an omnidirectional mobile robot, Mechatronics 26 (0) (2015) 36 – 44.

[25] E. Hashemi, M. G. Jadidi, N. G. Jadidi, Model-based pi-fuzzy control of four-wheeled omni-directional mobile robots, Robotics and Autonomous Systems 59 (11) (2011) 930 – 942.

[26] M. Najariyan, M. H. Farahi, A new approach for the optimal fuzzy linear time invariant controlled system with fuzzy coefficients, Journal of Computational and Applied Mathematics 259, Part B (0) (2014) 682 – 694.

[27] M. Mazandarani, M. Najariyan, Differentiability of type-2 fuzzy number-valued functions, Communications in Nonlinear Science and Numerical Simulation 19 (3) (2014) 710 – 725.

[28] J. Angeles, Fundamentals of Robotic Mechanical Systems, 4th Edition, Springer, 2014.

[29] P. Hsu, S. Sastry, The effect of discretized feedback in a closed loop system, in: Proc. of the IEEE Conference on Decision and Control (CDC), Vol. 26, 1987, pp. 1518–1523.

[30] S. Monaco, D. Normand-Cyrot, Advanced tools for nonlinear sampled-data systems' analysis and control, mini-tutorial, European Journal of Control 53 (2007) 221 – 241.

[31] T. Chen, B. Francis, Optimal sampled-data control systems, Springer-Verlag, Berlin, Germany, 1995.

[32] A. Astolfi, D. Nešić, A. Teel, Trends in nonlinear control, in: Decision and Control, 2008. CDC 2008. 47th IEEE Conference on, 2008, pp. 1870–1882.

[33] K. Åström, B. Wittenmark, Computer Controlled Systems, 3rd Edition, 3rd Edition, Prentice Hall, 1997.

[34] D. Nešić, A. Teel, A framework for stabilization of nonlinear sampled-data systems based on their approximate discrete-time models, IEEE Trans. on Automatic Control 49 (7) (2004) 1103–1122.

[35] D. S. Laila, D. Nešić, Changing supply rates for input-output to state stable discrete-time nonlinear systems with applications, Automatica 39 (5) (2003) 821 – 835.

[36] D. Nešić, L. Grüne, Lyapunov-based continuous-time nonlinear controller redesign for sampled-data implementation, Automatica 41 (7) (2005) 1143–1156.

[37] A. Savran, Discrete state space modeling and control of nonlinear unknown systems, ISA Transactions 52 (6) (2013) 795 – 806.

[38] M. Lemmon, Event-triggered feedback in control, estimation, and optimization, in: A. Bemporad, M. Heemels, M. Johansson (Eds.), Networked Control Systems Lecture Notes, Vol. 405 of Control and Information Sciences Networked Control Systems, Springer-Verlag, 2010, pp. 293–358.

[39] S. Hu, D. Yue, Event-triggered control design of linear networked systems with quantizations, ISA Transactions 51 (1) (2012) 153 – 162.

[40] K.-E. Årzén, A simple event-based PID controller, in: Proc. of the World Congress, The International Federation of Automatic Control (IFAC), Beijing, P.R. China, 1999.

[41] S. Durand, N. Marchand, Further results on event-based PID controller, in: Proc. of the European Control Conference (ECC), 2009.

[42] A. Ruiz, J. E. Jiménez, J. Sánchez, S. Dormido, A practical tuning methodology for event-based PI control, Journal of Process Control 24 (1) (2014) 278 – 295.

[43] J. Sánchez, M. Guarnes, S. Dormido, A. Visioli, Comparative study of event-based control strategies: An experimental approach on a simple tank, in: Proc. of the European Control Conference (ECC), 2009.

[44] W. Heemels, J. Sandee, P. van den Bosch, Analysis of event-driven controllers for linear systems, International journal of control 81 (2009) 571–590.

[45] J. Lunze, D. Lehmann, A state-feedback approach to event-based control, Automatica 46 (2010) 211–215.

[46] M. Velasco, P. Martí, E. Bini, On Lyapunov sampling for event-driven controllers, in: Proc. of the IEEE Conference on Decision and Control (CDC), 2009.

[47] P. Tabuada, Event-triggered real-time scheduling of stabilizing control tasks, IEEE Trans. on Automatic Control 52 (9) (2007) 1680–1685.

[48] A. Anta, P. Tabuada, Self-triggered stabilization of homogeneous control systems, in: Proceedings of the IEEE American Control Conference, 2008.

[49] N. Marchand, S. Durand, J. F. Guerrero-Castellanos, A general formula for event-based stabilization of nonlinear systems, IEEE Trans. on Automatic Control 58 (5) (2013) 1332–1337.

[50] N. Marchand, J. Martinez Molina, S. Durand, J. F. Guerrero-Castellanos, Lyapunov event-triggered control: a new event strategy based on the control, in: Proceedings of the 9th IFAC Symposium on Nonlinear Control Systems, 2013.

[51] R. C. Francy, A. M. Farid, K. Youcef-Toumi, Event triggered state estimation techniques for power systems with integrated variable energy resources, ISA Transactions 56 (0) (2015) 165 – 172.

[52] S. Durand, J. Minet, J. Guerrero-Castellanos, N. Marchand, AsynCar, a radio-controlled vehicle for asynchronous experiments: Implementation of an event-

based cruise control, in: Proceedings of the 8th IEEE International Conference on Electrical Engineering, Computing Science and Automatic Control, 2011.

[53] M. Guinaldo, E. Fabregas, G. Farias, S. Dormido-Canto, D. Chaos, J. Sánchez, S. Dormido, A mobile robots experimental environment with event-based wireless communication, Sensors 13 (7) (2013) 9396–9413.

[54] M. Jankovic, R. Sepulchre, P. V. Kokotovic, CLF based designs with robustness to dynamic input uncertainties, Systems & Control Letters 37 (1) (1999) 45 – 54.

[55] E. D. Sontag, Mathematical control theory, deterministic finite dimensional systems, 2nd Edition, Springler Verlag, New York Berlin Heidelberg, 1998.

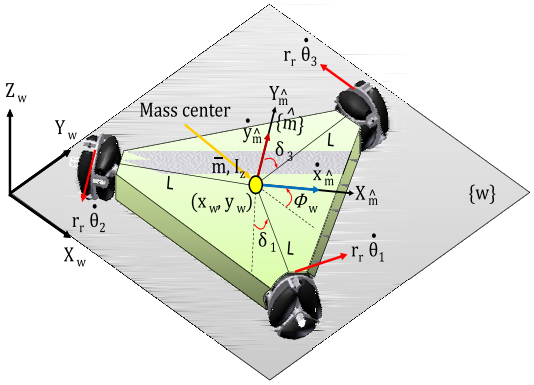

a)

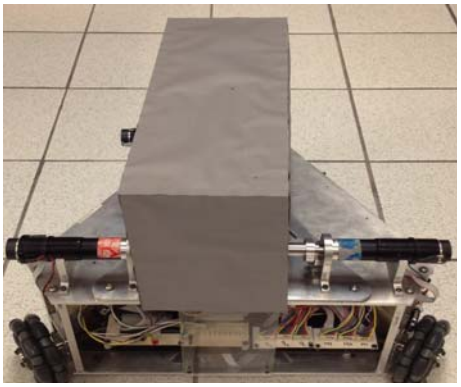

b)

Figure 1: Schematic diagram and photo of the (3,0) mobile robot.

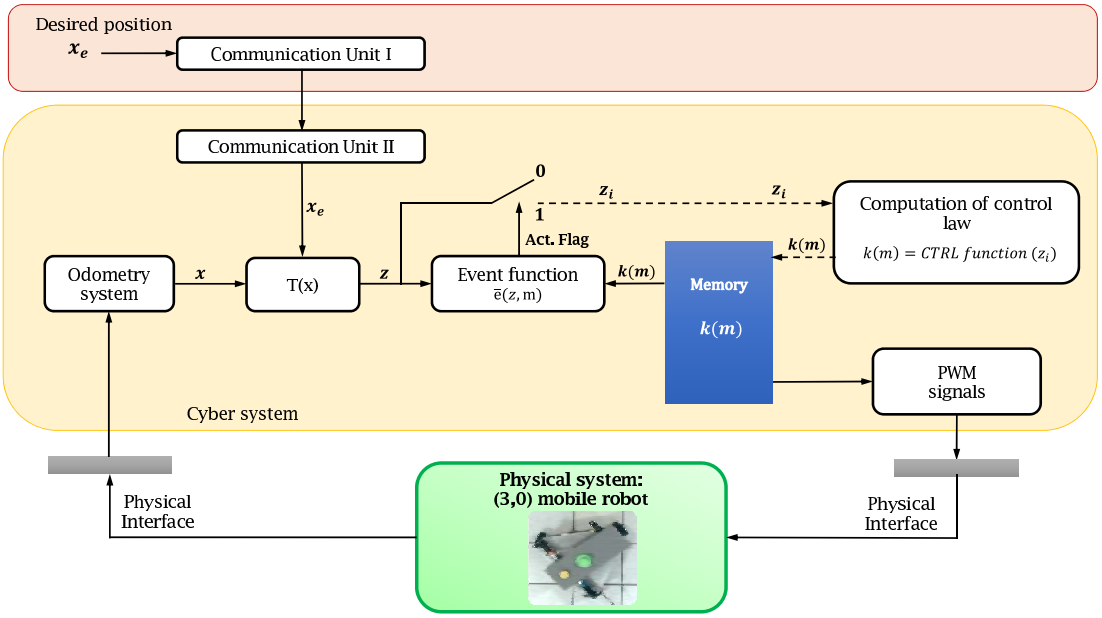

Figure 2: Schematic diagram of the event-triggered control system.

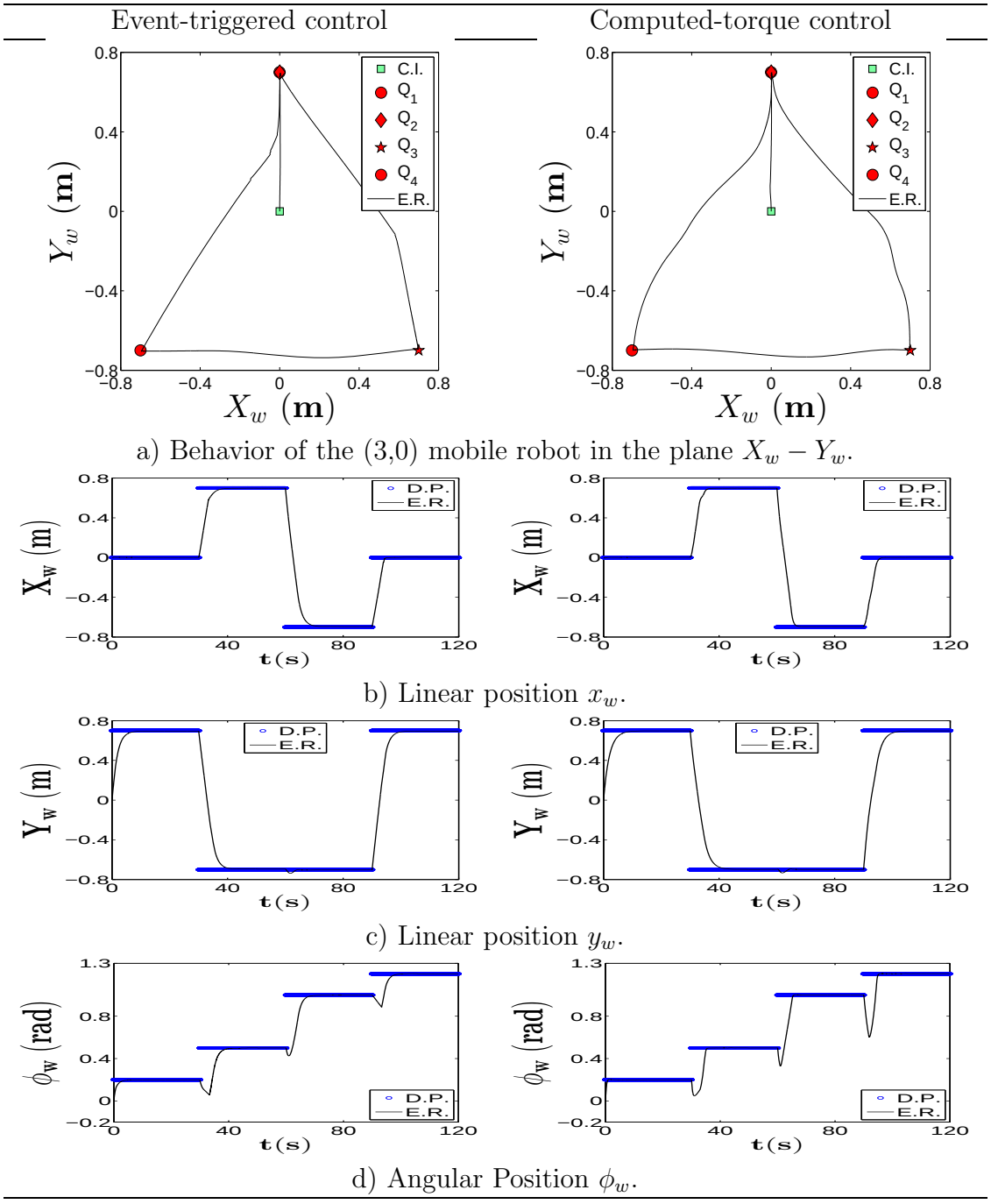

Figure 3: Comparative behavior between the event-triggered control and the computed-torque control in the stabilization problem of the (3,0) mobile robot. D.P.: Desired point (Q_1, Q_2, Q_3, Q_4). E. R.: Experimental results.

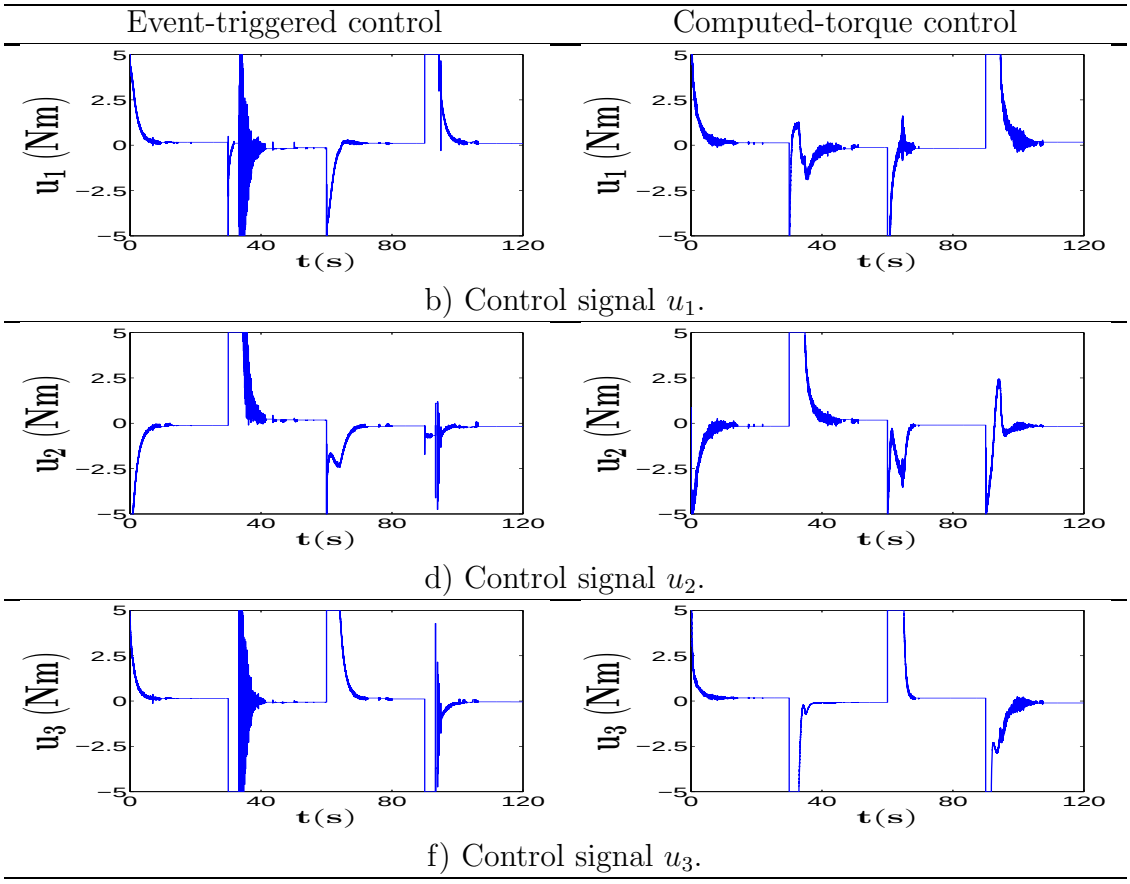

b) Control signal u_1.

d) Control signal u_2.

f) Control signal u_3.

Figure 4: Comparative control performance between the event-triggered control and the computed-torque control in the stabilization problem of the (3,0) mobile robot.

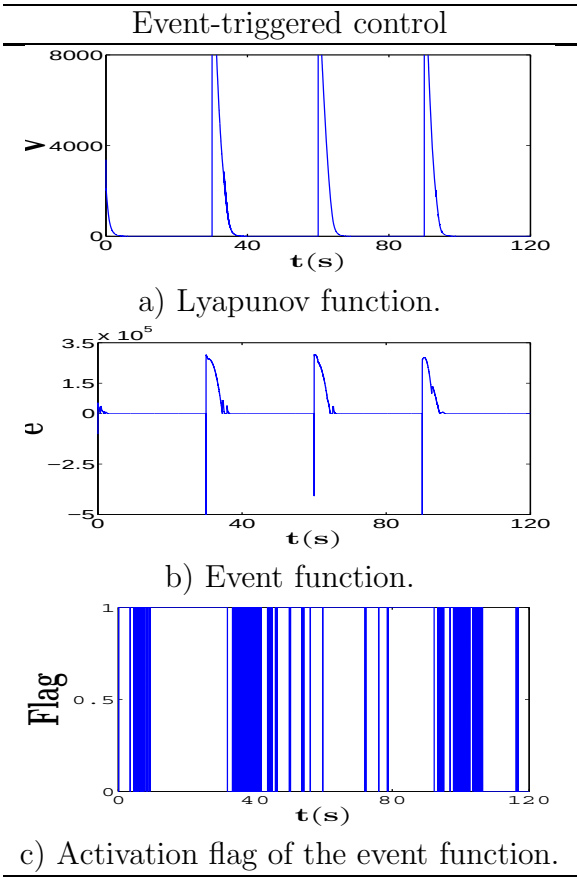

Figure 5: Lyapunov function V, event function $\bar{e}$ and activation flag for the event-triggered control in the stabilization problem of the (3,0) mobile robot.

Table I: Omnidirectional mobile robot specifications.

Parameter	**Description**	**Value**	**Units**
δ_1	Angle 1	$\pi/6$	rad
δ_2	Angle 2	$\pi/3$	rad
J	Wheel's inertia	5.82E-4	kg·m^2
I_z	Mobile's inertia	0.0127	kg·m^2
$\bar{m}$	Mass	11.83	kg
r	Wheel's radius	0.0625	m
L	Wheel's distance	0.287	m

Table II: Comparative results of the Event-Trigger Control and Computed Torque Control.

Control	IAE [m or rad]			ITAE [m s or rad s]			ISE [m^2 or rad^2]			$\sum_{\forall\, t}(\lvert u_1(t)\rvert + \lvert u_2(t)\rvert + \lvert u_3(t)\rvert)$ [Nm]
approach	x_w	y_w	ϕ_w	x_w	y_w	ϕ_w	x_w	y_w	ϕ_w	
ETC	7.47	10.36	5.93	462.48	558.66	333.50	4.86	7.87	2.01	47850.33
CTC	7.56	10.65	5.96	473.91	572.76	370.27	5.04	7.70	2.62	48044.85

List of figure captions:

Figure 1: Schematic diagram and photo of the (3,0) mobile robot.

Figure 2: Schematic diagram of the event-triggered control system.

Figure 3: Comparative behavior between the event-triggered control and the computed-torque control in the stabilization problem of the (3,0) mobile robot. D.P.: Desired point (Q_1, Q_2, Q_3, Q_4). E. R.: Experimental results.

Figure 4: Comparative control performance between the event-triggered control and the computed-torque control in the stabilization problem of the (3,0) mobile robot.

Figure 5: Lyapunov function V, event function $\bar{e}$ and activation flag for the event-triggered control in the stabilization problem of the (3,0) mobile robot.

List of table captions:

Tabla I: Omnidirectional mobile robot specifications

Tabla II: Comparative results of the Event-Trigger Control and Computed Torque Control.